Displays 35 (2014) 165–170

Contents lists available at ScienceDirect

Displays

journal homepage: www.elsevier.com/locate/displa

Electrical characteristics of amorphous In–Ga–Zn–O thin-film transistors prepared by radio frequency magnetron sputtering with varying oxygen flows

Yih-Shing Lee [a,*], Tung-Wei Yen [b], Cheng-I Lin [b], Horng-Chih Lin [b], Yun Yeh [c]

[a] Department of Optoelectronic System Engineering, Minghsin University of Science & Technology, Hsin-Fong, Hsin-Chu 30401, Taiwan, ROC
[b] Institute of Electronics & Department of Electronic Engineering, National Chiao Tung University, Hsin-Chu 300, Taiwan, ROC
[c] Institute of Electronics, Minghsin University of Science and Technology, Hsin-Chu 30401, Taiwan, ROC

ARTICLE INFO

Article history:
Received 18 April 2013
Received in revised form 30 March 2014
Accepted 7 May 2014
Available online 20 May 2014

Keywords:
Amorphous indium–gallium–zinc oxide (a-IGZO)
Oxygen flow
Carrier concentration
Total resistance method
Composition

ABSTRACT

This study investigates impacts of oxygen flow during the deposition of amorphous indium–gallium–zinc oxide (a-IGZO) channel layer with a radio frequency (r.f.) magnetron sputter on the electrical characteristics of the fabricated thin-film transistors (TFTs). Results indicate that as the film was deposited with a higher oxygen flow, the transfer curves are positively shifted while the field-effect mobility (μ_{FE}) is significantly decreased. To get more insight about the effects, channel resistance (R_{CH}) and the parasitic source-to-drain resistance (R_{SD}) of the fabricated devices are extracted using the total resistance method. The extracted a-IGZO channel resistance per unit length (r_{ch}) and R_{SD} are found to increase while the extracted effective mobility (μ_E) is decreased with increasing oxygen flow during sputtering. These observations are postulated to be related the decrease in the In/(In + Ga + Zn) ratio and the increase in the Zn/(In + Ga + Zn) ratio of the a-IGZO films with increasing the oxygen flow rate which lead to higher resistivity and lower carrier concentration. The extracted R_{SD} can be comparable with R_{CH} for the devices prepared with high oxygen flow, resulting in the roll-off of μ_{FE} as the channel length is shorter than 20 μm.

1. Introduction

Transparent amorphous oxide semiconductors (TAOSs) are promising for channel materials of thin-film transistors [1] (TFTs) and are feasible for driving TFTs in organic light-emitting diode displays due to large carrier mobility (>10 $cm^2 V^{-1} s^{-1}$| and low process temperatures. Amorphous indium–gallium–zinc oxide (a-IGZO) channel layers are usually deposited by sputters because of the low deposition temperature and thus the feasibility for manufacturing of devices on flexible substrates. It is well known that the properties of amorphous metal oxide semiconductor materials are strongly dependent on the processing conditions [2,3]. In this regard, there had been several reports exploring the effects of deposition power [2], oxygen flow [2,3] and working pressure [3,4], on the basic electrical characteristics of a-IGZO TFTs. Both direct current (d.c.) [5,6] and radio frequency (r.f.) sputters [3,7,8] have been adopted to deposit a-IGZO films and used as the channel in the fabrication of a-IGZO TFTs. In essence, to optimize the quality of a-IGZO film is important to achieve excellent device characteristics of a-IGZO TFTs. Recently, Kwon et al. [9] reported that the proposed oxygen incorporation calculation method and elucidates quantitative calculation of oxygen incorporation in sputtered IGZO films and the impact on a-IGZO transistor properties, the resistivity curve with O_2/IGZO incorporation ratio can be used for the tool to estimate the IGZO sputtering conditions for optimum TFT performance was confirmed. Shimura et al. [10] reported that the TFT performance varies with the source/drain materials since the source-to-drain current was found to be dependent on the contact resistance between the a-IGZO channel and source/drain (S/D) metals. In addition, the passivation layer which directly contact with the channel film region, such as hydrogenated silicon nitride (SiN_x), would highly reduce the channel resistivity by enhancing carrier concentration and forming nearly ohmic contacts to reduce the parasitic source to drain resistance [11]. Furthermore, argon (Ar) plasma treatment at source and drain metal contact regions in a-IGZO channel film also improve the contact resistance [12]. As a common understanding, the a-IGZO TFT is in general sensitive to the oxygen vacancy, however there is fewer reports demonstrating effects of a-IGZO channel resistance and S/D contact resistance with the channels deposited at various oxygen flows on electrical characteristics of a-IGZO devices.

* Corresponding author. Tel.: +886 3 5593142 3383; fax: +886 5593142 3388.
E-mail address: yslee@must.edu.tw (Y.-S. Lee).

http://dx.doi.org/10.1016/j.displa.2014.05.005
0141-9382/

This paper reports the impacts of oxygen flow during the deposition of a-IGZO channel layer with an r.f. magnetron sputter on the electrical characteristics of the fabricated TFTs with various channel lengths. Optimum electrical properties were indicated as the film was deposited with a lower oxygen flow from transfer and output characteristics. To get more insight about the effects, channel resistance (R_{CH}) and the parasitic source-to-drain resistance (R_{SD}) of the fabricated devices with various oxygen flows are extracted using the total resistance method [10,11]. Finally, the relationship between the metallic atomic ratio in a-IGZO films by X-ray photoelectron spectroscope (XPS) compositional analyses and the extracted a-IGZO channel resistance per unit length (r_{ch}), the parasitic source-to-drain resistance (R_{SD}), and effective mobility (μ_E) were explained.

2. Experiments

The composition of the IGZO powder used in the experiment was mixed by an atomic ratio of In:Ga:Zn = 1:1:1. The target powder (In_2O_3, Ga_2O_3, ZnO) with high purity were more than 99.99%. After the IGZO target was formed and sintered, we mounted it in

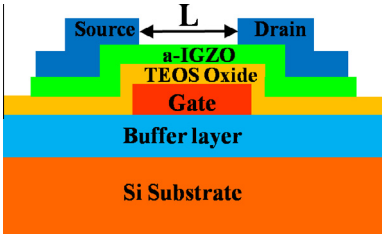

Fig. 1. The cross-sectional view of the fabricated a-IGZO TFTs device.

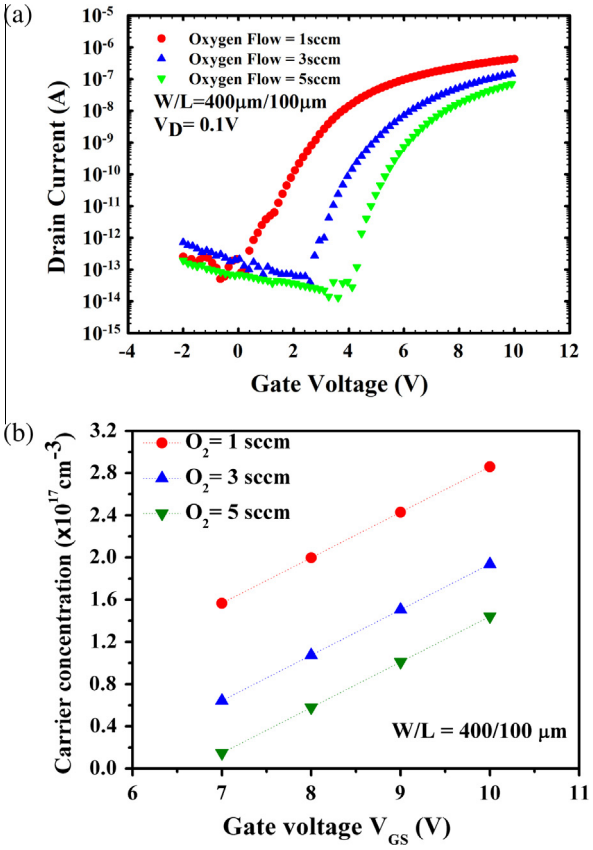

Fig. 2. (a) Typical transfer curves and (b) estimated carrier concentration (n) of the channel of a-IGZO TFTs at W/L = 400/100 μm as a function of gate voltage for each oxygen flow.

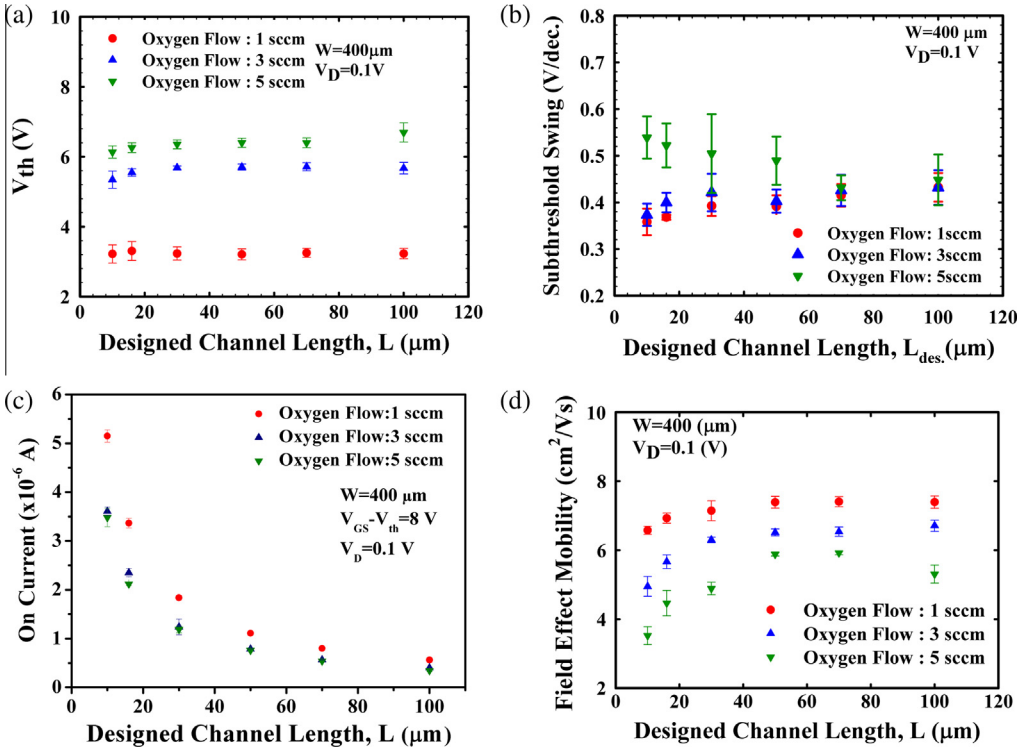

Fig. 3. (a) Extracted threshold voltage (V_{th}), (b) sub-threshold swing (SS), (c) on-current measured at $V_{GS} - V_{th}$ = 8 V, and (d) field-effect mobility (μ_{FE}) of a-IGZO devices deposited with various oxygen flows as a function of L. All values are V_D = 0.1 V data.

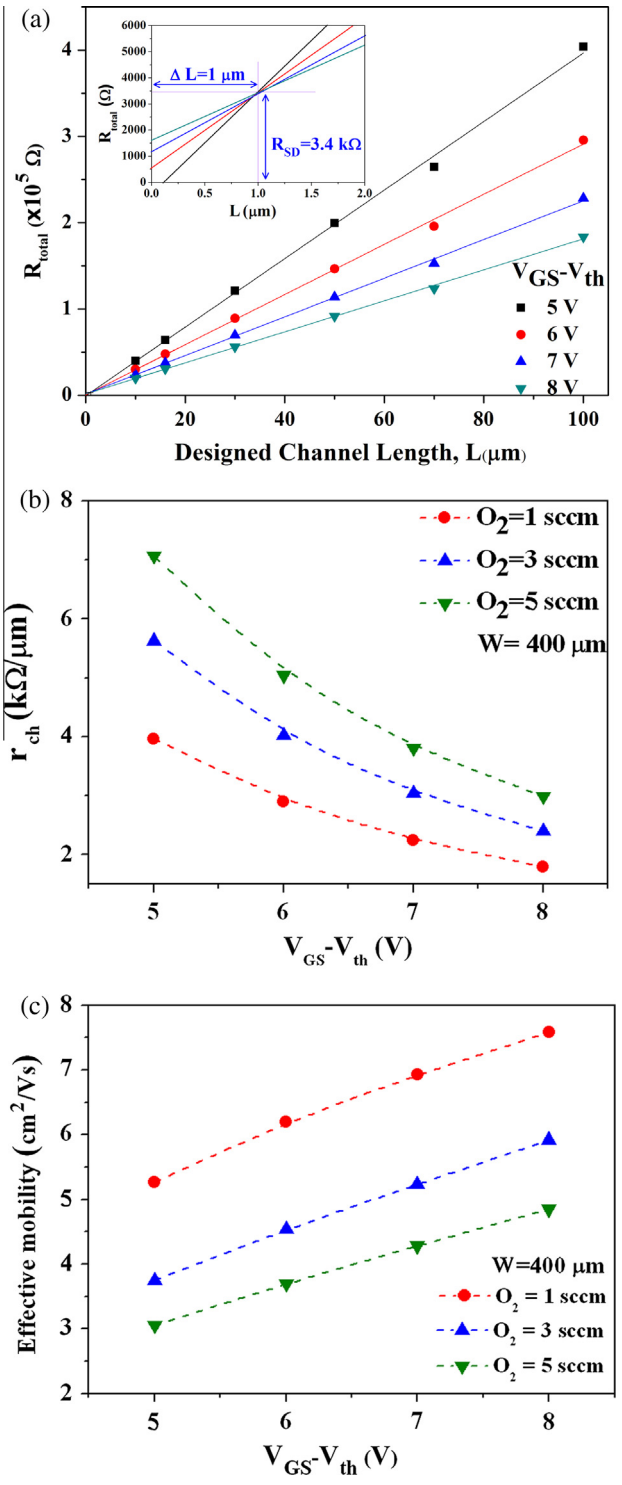

Fig. 4. (a) Dependences of $R_{total} - L$ of a-IGZO devices deposited with an oxygen flow rate at 1 sccm and W = 400 μm characterized at V_D = 0.1 V and $V_{GS} - V_{th}$ = 5–8 V. The inset shows a magnified view in the small L to depict the point of intersection. (b) Channel resistance per channel length (r_{ch}) and (c) effective mobility (μ_E) of a-IGZO devices deposited with various oxygen flows as a function of gate overdrive.

the sputter chamber for the deposition of IGZO thin films on glass substrates. The film thicknesses of the a-IGZO thin film were determined in the wavelength range of 200–900 nm using an n&k analyzer 1200 (n&k Technology). The atom ratio of the deposited a-IGZO films with the various oxygen flows was investigated by XPS. Fig. 1 shows the cross-sectional schematic structure of the a-IGZO TFTs device. A 200 nm Al–Si–Cu was first deposited by physical vapor deposition (PVD) on a 4″ silicon substrate capped with 500 nm-thick thermally grown silicon dioxide (SiO_2) film. The metal layer was patterned by photolithographic and subsequent wet etching steps to form the gate electrode. Then, a 100 nm TEOS oxide was deposited by plasma-enhanced chemical vapor deposition (PECVD) as the gate dielectric. Before depositing the a-IGZO active layer, we had to pre-sputter the target for 15 min to prevent the contamination of IGZO target surface. Subsequently, a 50 nm a-IGZO film was deposited as the channel layer by the r.f. sputter with varied oxygen partial pressure at room temperature under a fixed deposition power of 100 W. The system's base and working pressures were 3×10^{-6} Torr and 5 m Torr, respectively. During sputtering, the flow rate of Ar was fixed at 50 standard cubic centimeter per minute (sccm), while the oxygen flow rate was set at 1 sccm, 3 sccm, or 5 sccm, with oxygen partial pressure of 9.8×10^{-5}, 2.83×10^{-4}, and 4.54×10^{-4} Torr, respectively. A 300 nm Al–1.5 wt% Ti S/D metal was then formed with a lift-off process. Afterwards, a lithographic step to define the active device region was performed. A diluted HCl solution ($HCl:H_2O$ = 1:200) was used instead to avoid damage and severe lateral etching of the a-IGZO channel film. In order to contact the gate electrode, contact etching was performed by wet etching using buffer oxide etcher (B.O.E.).

The channel width (W) was fixed at 400 μm and the designed channel length (L), which is defined as the distance between the source and drain metal pads, was varied from 10 μm to 100 μm. Electrical measurements of all devices were executed by an Agilent 4156A precision semiconductor parameter analyzer, and the measurement temperature was maintained at 25 °C. Prior to the measurements, all a-IGZO TFTs samples used in this study were annealed at 200 °C in air for 40 min on the hot plate aiming to remove the excess moisture on TFTs. For a low V_D (at 0.1 V), the total resistance (R_{total}) as a function of the designed channel length can be evaluated by using the total resistance method conducted in the linear region of the output characteristic of the devices [11,13]:

$$R_{total} = \frac{V_D}{I_D} = r_{ch}(L - \Delta L) + R_{SD} \quad (1)$$

$$r_{ch} = \frac{1}{\mu_E C_{OX} W (V_{GS} - V_{th})} \quad (2)$$

$$R_{total} = R_{CH} + R_{SD} \quad (3)$$

where r_{ch} is the channel resistance per channel length, R_{CH} and R_{SD} are the channel resistance and S/D parasitic resistance, respectively; C_{ox} is the oxide capacitance per unit area, the channel width (W) and the designed channel length (L) were determined by the size of the S/D pad mask, $\Delta L = L - L_{eff}$, L_{eff} is the effective channel length, V_{th} is the threshold voltage defined as the gate voltage when the current is a constant ($10^{-9} \times (W/L)$A) and μ_E is the effective mobility. From Eqs. (1) and (2), we can evaluate r_{ch} and μ_E as a function of gate overdrive, respectively; R_{SD} can be extracted from Eq. (1) and R_{CH} can be calculated from Eq. (3).

3. Results and discussion

Fig. 2(a) shows the typical transfer curves of a-IGZO TFTs samples with various oxygen flows at W/L = 400/100 μm. Oxygen vacancies are the main source to release free electrons to transport in the metal-oxide semiconductors. This is clearly confirmed in the figure that the transfer curves are positively shifted with increasing the oxygen flow. Therefore, a higher gate voltage is necessary to accumulate free electrons to form a conductive layer between the source and drain. The carrier concentration induced by the gate

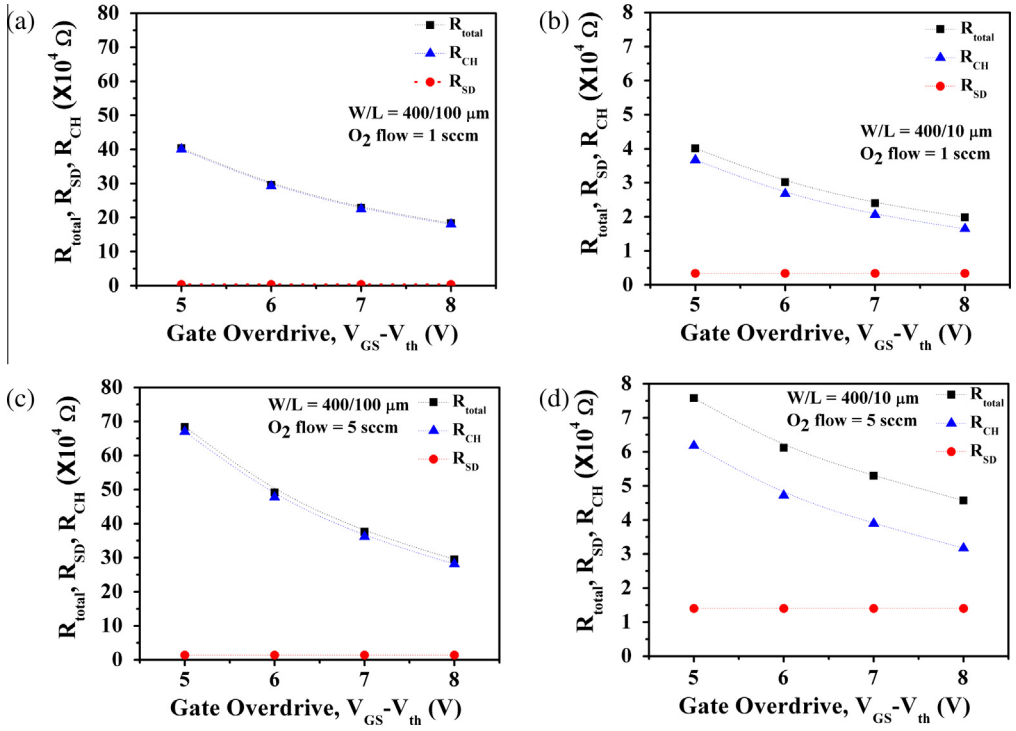

Fig. 5. R_{total}, R_{ch}, and R_{SD} as a function of gate overdrive for devices with (a) W/L = 400/100 μm and (b) W/L = 400/10 μm prepared with an oxygen flow rate of 1 sccm, and devices with (c) W/L = 400/100 μm and (d) W/L = 400/10 μm prepared with an oxygen flow rate of 5 sccm.

voltage at the interface of the a-IGZO semiconductor film and the insulator (in cm^{-3}) can be estimated by the followings [13,14]:

$$r_{ch} = \frac{1}{\mu_E enWt} = \frac{1}{\mu_E C_{OX} W(V_{GS} - V_{th})} \quad (4)$$

$$n = \frac{C_{OX}(V_{GS} - V_{th})}{et} \quad (5)$$

where e is the elementary charge, n is an estimated carrier concentration of the a-IGZO channel, and t is the channel thickness. Fig. 2(b) shows the estimated carrier concentration (n) of the a-IGZO channel as a function of gate voltage for each oxygen flow at W/L = 400/100 μm. The estimated carrier concentration increased with increasing the gate voltage, and the a-IGZO channel layer deposited with a lower oxygen flow tends to enhance the carrier concentration in the channel ascribed to a smaller V_{th}. The extracted V_{th}, sub-threshold swing (SS), on-current, and field-effect mobility (μ_{FE}) of a-IGZO devices deposited with various oxygen flows are shown as a function of L in Fig. 3(a–d) respectively. Fig. 3(a) shows that the V_{th} has a weak dependence on the channel length. This is because the channel length is more than 30 times larger than the gate oxide thickness, thus the short channel effects are expected to be small. In addition, it is seen that the variation of V_{th} is increased with increasing oxygen flow. In Fig. 3(b), the SS increases with increasing oxygen flow. It is known that the SS can be affected by the bulk defects in the a-IGZO channel film in addition to the interface traps, thus the reduction in SS might result from the greater densification and lower amount of the bulk defects as deposited at a lower oxygen partial pressure [2–4]. Fig. 3(c) shows the on-current measured under the same gate overdrive voltage of 8 V. As shown in Fig. 3(c), the on-current reduces with increasing oxygen flow owing to deficiency in the estimated carrier concentration, as shown in Fig. 2(b). Fig. 3(d) shows that μ_{FE} is dependent on the channel length. The μ_{FE} for the devices processed at a higher oxygen flow rate is obviously reduced as the channel length is shorter than 20 μm. It is postulated to be related to the effect of the S/D parasitic resistance in these devices with a shorter channel length. Next, this issue is clarified by measuring the resistance components in the devices.

Fig. 4(a) shows the dependences of $R_{total} - L$ of a-IGZO devices of W = 400 μm deposited with the oxygen flow rate of 1 sccm characterized at V_D = 0.1 V and $V_{GS} - V_{th}$ = 5–8 V. According to Eq. (1), R_{SD} = 3.4 kΩ and ΔL = 1.0 μm are determined, as shown in the inset of Fig. 4(a). The shrinkage of the channel length, ΔL = 1.0 μm would be attributed to the critical-dimension loss of the S/D metal spacing resulted during the corresponding lithographic and following lift-off process steps. In addition, the respective R_{SD} values extracted using the above procedure are 3.4, 3.9, and 14 kΩ for splits with oxygen flow rate of 1, 3, and 5 sccm, respectively. Results of the extracted channel resistance per channel length (r_{ch}) and the effective mobility (μ_E) of a-IGZO devices with various oxygen flows as a function of gate overdrive are shown in Fig. 4(b) and (c), respectively. It is obvious that a higher gate overdrive voltage induces more free electrons to transport in the channel, which is the main reason for the lowering in channel resistance. Because the a-IGZO channel layer deposited with a higher oxygen flow tends to reduce the carrier concentration in the channel, a higher potential barrier height and longer transport paths are expected from the percolation model [15]. This well explains the findings shown in Fig. 4(b) and (c) that r_{ch} is higher while μ_E is lower in the films deposited with a higher oxygen flow at the same gate overdrive voltage. Extracted R_{total}, R_{CH}, and R_{SD} as a function of gate overdrive with the L = 100 μm and 10 μm for the a-IGZO TFT devices with oxygen flow rates of either 1 or 5 sccm are shown in Fig. 5. As can be seen in Fig. 5(a) and (b), for the low oxygen flow rate of 1 sccm, the R_{SD} contribution to R_{total} is negligible regardless of the channel length and studied gate overdrive. On the other hand, for the devices prepared with the oxygen flow of 5 sccm, the R_{SD} contribution to R_{total} is still mild as with a long channel (L = 100 μm), as shown in Fig. 5(c). However, as the channel length is shortened to 10 μm, the impact of the R_{SD} on device characteristics is no longer negligible, as shown in Fig. 5(d). Actually R_{SD} is

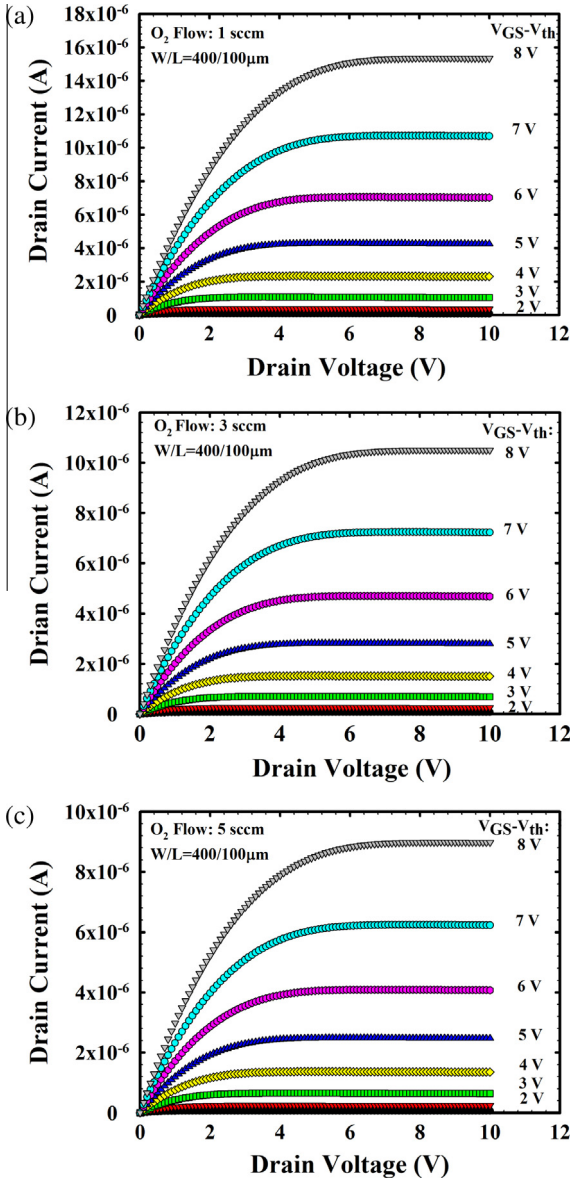

Fig. 6. Output characteristic of a-IGZO devices at $W/L = 400/100\ \mu m$ with the channel film deposited at an oxygen flow of (a) 1 sccm, (b) 3 sccm, and (c) 5 sccm.

comparable with R_{ch}, as shown in the figure. This observation also reasonably explains the trend shown in Fig. 3(d) that noticeable decline in μ_{FE} as the channel length is shorter than 20 μm for the devices with oxygen flow of 5 sccm. Similar finding was also reported by Barquinha et al. [16]. Fig. 6 shows the output characteristics of devices with the channel film deposited at different oxygen flows and $W/L = 400/100\ \mu m$. The saturation current at the same gate overdrive obviously decreases with the higher oxygen flow. Despite the higher resistivity, the ohmic S/D contacts are

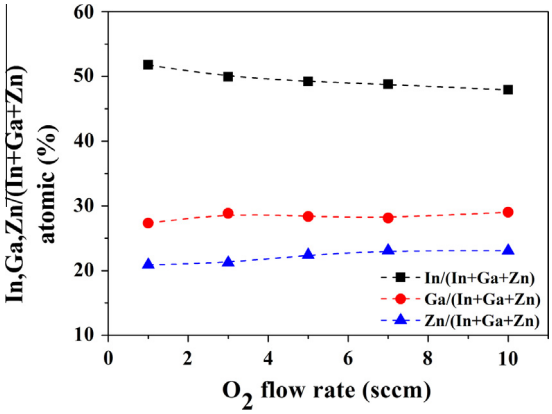

Fig. 7. In, Ga, and Zn/(In + Ga + Zn) atomic ratios for the deposited a-IGZO films as a function of the oxygen flow rate.

still formed for the split with high oxygen flow as shown in the output characteristics, attributed to the S/D parasitic contact resistance is negligible for a-IGZO TFT devices with $W/L = 400/100\ \mu m$ from Fig. 5(c).

Fig. 7 shows the measured In, Ga, and Zn/(In + Ga + Zn) atomic ratios for the deposited a-IGZO films with various oxygen flows. The results were obtained with the XPS technique. By increasing oxygen flow rate from 1 to 10 sccm, the value of In/(In + Ga + Zn) ratio of the deposited films decreases from 51.8% to 47.9%, but the values of Ga/(In + Ga + Zn) and Zn/(In + Ga + Zn) ratios of them increase from 27.3% to 29.0% and from 20.9% to 23.1%, respectively. The dependence of the In/(In + Ga + Zn) and Ga/(In + Ga + Zn) ratios on the oxygen flow rate is postulated to have strong influences on device characteristics including V_{th}, μ_{FE}, carrier concentration and off current, same relationships between electrical properties and metal oxide compositions have been reported by some Refs. [8,16]. Previous studies [18,19] have also shown that the resistivity of a-IGZO films was higher with a higher zinc atomic ratio. Moreover, it has been reported that an increase in Zn/(In + Ga + Zn) ratio with the oxygen flow rate tends to cause an increase in V_{th} [8], similar findings in our study. Typical values including the channel resistance per channel length (r_{ch}), effective mobility (μ_E) at $V_{gs}-V_{th} = 8$ V, estimated carrier concentration (n) at $V_{gs} = 10$ V, and threshold voltage (V_{th}) of a-IGZO TFTs at $W/L = 400/100\ \mu m$; In/(In + Ga + Zn), Ga/(In + Ga + Zn), and Zn/(In + Ga + Zn) atomic ratios of the deposited a-IGZO films for each oxygen flow are summarized in Table 1. r_{ch} is higher while μ_E is lower in the films prepared with a higher oxygen flow. Meanwhile, threshold voltage of a-IGZO devices increased from 3.37 to 6.66 V with increasing the oxygen flow rate. They are postulated to be related the decrease in the carrier concentration in the channel, owing to the reduction of the In/(In + Ga + Zn) ratios and the increase of Zn/(In + Ga + Zn) ratio of the a-IGZO films with the oxygen flow rate. In addition, the parasitic source-to-drain resistance, R_{SD} obviously increases with increasing the oxygen flow rate from 3.4 kΩ to 14 kΩ, however R_{SD} would not depend on the carrier concentration in the channel because it is not changed by a different gate overdrive voltage.

Table 1
Extracted channel resistance per channel length (r_{ch}), effective mobility (μ_E) at $V_{gs} - V_{th} = 8$ V, estimated carrier concentration (n) at $V_{gs} = 10$ V, and threshold voltage (V_{th}) of a-IGZO TFTs at $W/L = 400/100\ \mu m$; In/(In + Ga + Zn), Ga/(In + Ga + Zn), and Zn/(In + Ga + Zn) atomic ratios of the deposited a-IGZO films for each oxygen flow.

O_2 flow (sccm)	r_{ch} (Ω/μm)	μ_E (cm^2/V-sec)	n (cm^{-3})	V_{th} (V)	In/(In + Ga + Zn) (%)	Ga/(In + Ga + Zn) (%)	Zn/(In + Ga + Zn) (%)
1	2059	7.58	2.86×10^{17}	3.37	51.8	27.3	20.9
3	2852	5.92	1.94×10^{17}	5.51	49.9	28.8	21.2
5	3468	4.85	1.44×10^{17}	6.66	49.2	28.4	22.4

4. Conclusions

Effects of various oxygen flows on the electrical characteristics of a-IGZO TFTs prepared by r.f. magnetron sputtering are explored in this work. With an increased oxygen flow rate, the transfer curves are positively shifted while μ_{FE} and on current (at a fixed gate overdrive) decrease owing to a reduction in the estimated carrier concentration of the channel. The estimated carrier concentration increased with decreasing oxygen flow tends to enhance μ_{FE}, and on-current, while reduced V_{th} of a-IGZO devices. This is confirmed by the results of the resistance measurements that r_{ch} is higher while μ_E is lower in the films prepared with a higher oxygen flow. These outcomes are postulated to be related the decrease of the In/(In + Ga + Zn) ratio and the increase of Zn/(In + Ga + Zn) ratio of the deposited a-IGZO films with increasing oxygen flow rate. Meanwhile, R_{SD} obviously increases from 3.4 kΩ to 14 kΩ when the oxygen flow rate increases from 1 to 5 sccm, however R_{SD} would not depend on the carrier concentration in the channel because it is not changed by a different gate overdrive voltage.

Acknowledgment

This work was supported by National Science Council Research Project (NSC 101-2221-E-159 -005-).

References

[1] K. Nomura, H. Ohta, A. Takagi, T. Kamiya, M. Hirano, H. Hosono, Nature 432 (2004) 488–492.
[2] P. Barquinha, L. Pereira, G. Gonçalves, R. Martins, E. Fortunato, Electrochem. Solid-State Lett. 11 (2008) H248–H251.
[3] P. Barquinha, L. Pereira, G. Gonçalves, R. Martins, E. Fortunato, J. Electrochem. Soc. 156 (2009) H161–H168.
[4] J.H. Jeong, H.W. Yang, J.S. Park, J.K. Jeong, Y.G. Mo, H.D. Kim, J. Song, C.S. Hwang, Electrochem. Solid-State Lett. 11 (2008) H157–H159.
[5] T. Aoi, N. Oka, Y. Sato, R. Hayashi, H. Kumomi, Y. Shigesato, Thin Solid Films 518 (2010) 3004–3009.
[6] Y.K. Moon, S. Lee, D.H. Kim, D.H. Lee, C.O. Jeong, J.W. Park, Jpn. J. Appl. Phys. 48 (2009) 031301-1–031301-4.
[7] H. Yabuta, M. Sano, K. Abe, T. Aiba, T. Den, H. Kumomi, Appl. Phys. Lett. 89 (2006) 112123-1–112123-3.
[8] T. Iwasaki, N. Itagaki, T. Den, H. Kumomi, K. Nomura, T. Kamiya, H. Hosono, Appl. Phys. Lett. 90 (2007) 242114-1–242114-3.
[9] S. Kwon, J.H. Noh, J. Noh, Philip D. Rack, J. Electrochem. Soc. 158 (2011) H289–H293.
[10] Y. Shimura, K. Nomura, H. Yanagi, T. Kamiya, M. Hirano, H. Hosono, Thin Solid Films 516 (2008) 5899–5902.
[11] A. Sato, K. Abe, R. Hayashi, H. Kumomi, K. Nomura, T. Kamiya, M. Hirano, H. Hosono, Appl. Phys. Lett. 94 (2009) 133502-1–133502-3.
[12] B.D. Ahn, H.S. Shin, H.J. Kim, J.S. Park, J.K. Jeong, Appl. Phys. Lett. 93 (2008) 203506-1–203506-3.
[13] D. Kang, H. Lim, C. Kim, I. Song, J. Park, Y. Park, Appl. Phys. Lett. 90 (2007) 192101-1–192101-3.
[14] S. Martin, C.S. Chiang, J.Y. Nahm, T. Li, J. Kanicki, Y. Ugai, Jpn. J. Appl. Phys. 40 (2A) (2001) 530–537.
[15] H. Hosono, J. Non-Cryst. Solids 352 (2006) 851–858.
[16] P. Barquinha, A.M. Vila, G. Gonçalves, L. Pereira, R. Martins, J.R. Morante, E. Fortunato, IEEE Trans. Electron Dev. 55 (4) (2008) 954–960.
[18] Y.S. Lee, W.J. Chen, J.S. Huang, S.C. Wu, Thin Solid Films 520 (2012) 6942–6946.
[19] Y.S. Lee, Z.M. Dai, C.I. Lin, H.C. Lin, Ceram. Int. 38S (2012) S595–S599.

Further reading

[17] J.K. Jeong, J.H. Jeong, H.W. Yang, J.S. Park, Y.G. Mo, H.D. Kim, Appl. Phys. Lett. 91 (2007) 113505-1–113505-3.